THE EFFECTS OF CLIMATE CHANGE ON THE PERFORMANCE OF ASPHALTIC PAVEMENT STRUCTURES

Carla Beatriz Costa de Araújo[1], Francisco de Assis de Souza Filho [2], Jorge Barbosa Soares[3] and Samuel Almeida Torquato e Silva[4]
[1]Department of Geology, Federal University of Ceara, Fortaleza, Brasil
carlabeatriz@ufc.br
[2]Department of Hydraulic and Environmental Engineering, Federal University of Ceara, Fortaleza, Brasil
assis@ufc.br
[3]Department of Transport Engineering, Federal University of Ceara, Fortaleza, Brasil
jsoares@det.ufc.br
[4]Department of Transport Engineering, Federal University of Ceara, Fortaleza, Brasil
samuel@det.ufc.br

ABSTRACT

An integrated climate-pavement model is presented to predict service performance. A total of 144 scenarios were considered from a combination of different pavement shoulder conditions (0.0 m; 0.5 m; 1.0 m; 1.5 m), water depth levels (3.0 m; 3.5 m; 4.0 m; 4.5 m), varied thicknesses of asphalt surface courses (2.0 cm; 5.0 cm; 10.0 cm), and three rainy periods (above average, below average, average), applicable to the Metropolitan Region of Fortaleza (MRF). In addition, it was considered the MRF climate change predictions for the 21st century (2031-2070) using 5 climate change models based on the CMIP5 (Coupled Model Intercomparison Project) RCP (Representative Concentration Pathways) scenarios 8.5 and 4.5. Without taking into account the climatic variability the performance analysis estimated a structural service life ranging from 1.0 to 5.6 years less, indicating that without the integrated methodology, the project is likely to be undersized. For MRF, the climate change models show that the average rainfall should decrease and years of above-average rainfall will be less frequent. In general, it was observed that the integrated methodology provides gains in the development of infrastructure projects and allows to predict how climate change scenarios may affect these projects.

KEYWORDS: *Climate change, Pavements, Performance & Design.*

I. INTRODUCTION

Climate change has been one of humanity's most strongly felt impacts on Earth's systems along with changing river courses, waterproofing areas, deforestation, construction of dams, among others ([1]; [2]). Conversely, both the climate and the water cycle have exerted strong impacts on anthropized environments, in part shaping the development of cities as factors such as droughts and floods, urban floods, heat islands, among others. According to [3], in some regions of the planet the terrestrial system is currently more influenced by anthropogenic effects than it is by natural ones. Human pressures have reached a state in which the continental hydrological and climatic cycles can no longer be considered part of the natural processes of terrestrial systems, hence the need to define a new era called the Anthropocene.

Cities and the different systems that compose them must be thought of as an integrated part of water and climate factors. In this context, it is important to use tools that allow an integrated analysis of civil infrastructures in an anthropized environment. These can help identifying the connections as well as developing more effective and robust plans and projects when recognizing the interconnections between the different subsystems.

Transport infrastructure is subject to changing weather, such as atmospheric precipitation and solar radiation. However, few studies in Brazil ([4]; [5]) incorporate all climatic variables to roadway design. [6] also point out that developing sustainable engineering projects requires sharing and obtaining information, through more collaborative research between climatologists and pavement engineers. In addition, available data on climate, paving, the economy, and the environment must be integrated into dynamic system models and used for long-term cost and performance forecasts.

Assuming stationary climate in roadway design can lead to totally incorrect performance prediction. [7] estimate in their research that anthropogenic climate change can result in rapid infrastructure failure and, consequently, higher maintenance costs of highways in the United States of America (USA). Other studies ([8]; [9]; [10]; [11]; [12]; [13]) reinforce the importance of updating engineering practice standards in the face of climate change.

However, incorporating climate projections into pavement design is not a trivial task. The integration of the most recent simulations of global climate models into pavement models is a complex challenge [13]. This work presents an analysis of the performance of asphalt pavements in the face of climate change using a simplified methodology for integrating climate variables and road infrastructures.

The work is structured in four sections (introduction, methodology, results and conclusions). In this first section, the main motivations and contributions of the research and the research objectives are presented. The methodology used in the research is described in the second chapter. All stages of development of the work are detailed, each of the models adopted is characterized, as well as all the hypotheses employed are presented. In the third section, the results obtained for the subsystem integration methodology are presented, as well as the analyzes for climate change for the study region. The research conclusions indicating the results obtained and the objectives achieved are presented in the fourth chapter.

II. METHODOLOGY

The purpose of this work is to analyze pavement design integrated with both climatic and hydrological variables, allowing a better understanding of pavement performance under current and future climatic characteristics. The methodology developed herein can be used in several regions and it is presented how it was applied in Fortaleza's Metropolitan Region (MRF), as depicted in Figure 1.

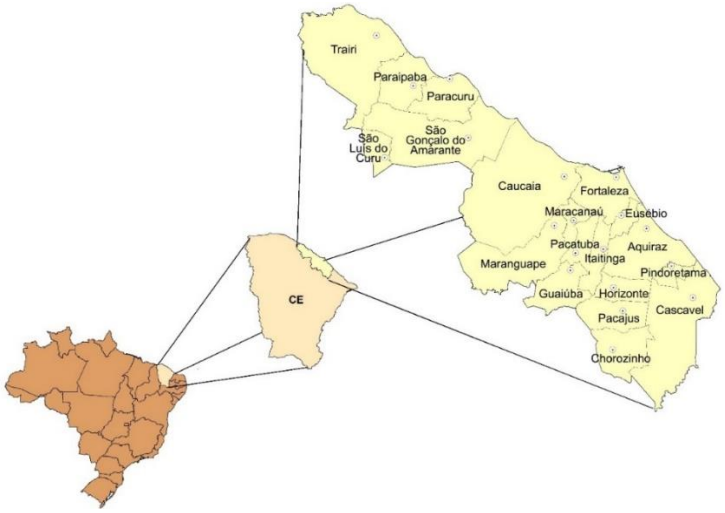

Figure 1. Metropolitan Region of Fortaleza

One of the main stages of the work was the definition of the general strategy, given that the structure of the roadway system is composed of a wide variety of materials, and that the climatic/hydrological systems exhibit different environmental conditions. Under these conditions, an integrated analysis

requires certain simplifications. To develop the proposed methodology, it was first identified and characterized each one of the following models:

- Climate model: precipitation for current climate, future climate, and temperature;

- Hydrological model: discharge and infiltration conditions in the hydrographic basin and over pavement structures;

- Transient flow model in unsaturated porous medium: characterization of the flow in the pavement layers;

- Floor stiffness model: variations in stiffness of the pavement layers, due to climatic variations.

Once the models were identified, it was necessary to understand how these different systems relate to one another and which are the most important variables for connecting them. Figure 2 shows the methodological scheme for the integrated design of roadway infrastructure. The climate model was used to extract information on precipitation (P) and temperature (T) of the region investigated. From the definition of the hydrological model, the flow and infiltration conditions (f) are characterized using rain data (P) as input. The response of the transient flow model in an unsaturated porous medium is the variation in moisture (Δu) in the different pavement layers, which occurs due to infiltration (f). The change in moisture (Δu) causes changes in the stiffness (resilient modulus, RM) of granular materials. Finally, these changes lead to variation in the performance of the infrastructures that can be estimated through mathematical models.

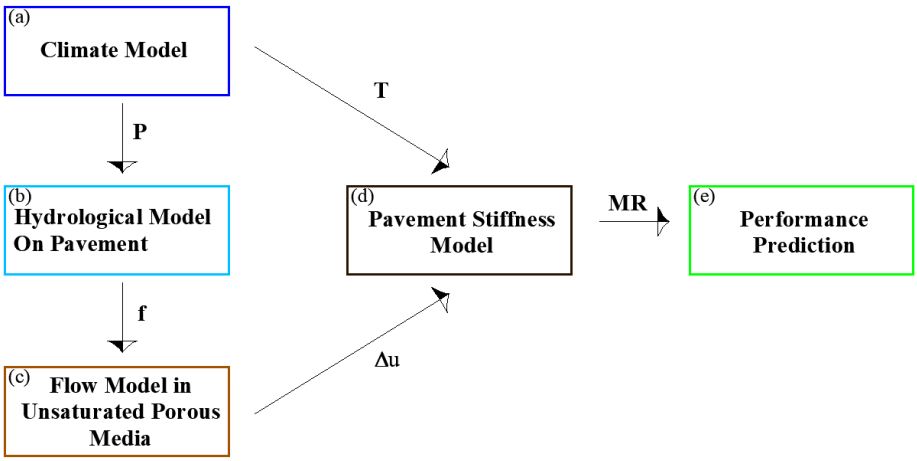

Figure 2. Methodological scheme for the integrated design of pavements

2.1. Climate Model

For the climate model, the main conditions analyzed were rainfall, considering both the current and the future climate. For the climate change models, five General Circulation Models (GCMs) were used for the studied region, considering the CMIP5 RCPs (Representative Concentration Pathways) 4.5 and 8.5 projections: (1) BCC-CM1 (Beijing Climate Center); (2) CanESM2 (Canadian Center for Climate Modeling and Analysis); (3) CESM1-CAM4 (National Center of Atmospheric Research); (4) inmcm4 (Institute for Numerical Mathematics Climate Model 4); and (5) MIROC5 (Japan Agency for Marine-Earth Science and Technology). These models were evaluated by [14] as accurately representing the patterns of variation in rainfall in the 20th century over the northern northeast of Brazil. Furthermore, they were used by both [15] and [10], and the latter group applied them in the city of Fortaleza.

For future climate projections, data was extracted from the CMIP5 website (http://cmippcmdi.llnl.gov/cmip5/). Monthly precipitation data was collected for the region, but was corrected using the gamma distribution, using bias adjustments ([16]; [17]) according to the following steps:

1st Step - Adjust the gamma distribution for the observed data;

2nd Step - Adjust the gamma distribution for models of the 20th century precipitation data to identify the problem by adjusting for bias;

3rd Step - Adjust the gamma distribution for the 21st century precipitation data models;

4th Step - Correct the estimates of the 20th and 21st century.

One of the analyses of the projections of the climate change models was the calculation of the anomalies of maximum, minimum, and average rainfall, all three measured through percentage variation and calculated as the difference of the XXI century scenario and the historical scenario, according to Equation 1:

$$A_{máx,mín,med} = \frac{P^{XXI}_{max,min,ave} - P^{XX}_{max,min,ave}}{P^{XX}_{max,min,ave}} . 100 \quad (1)$$

Where: A_{max} = maximum precipitation anomaly; P^{XXI}_{max} = maximum precipitation for the century scenario XXI; P^{XX}_{max} = maximum precipitation for the historical scenario; A_{min} = anomaly of minimum precipitation; P^{XXI}_{min} = minimum rainfall for the century scenario XXI; P^{XX}_{ave} = average precipitation for the historical scenario; A_{ave} = average precipitation anomaly; P^{XXI}_{ave} = average precipitation for the century scenario XXI; P^{XX}_{ave}= average rainfall for the historical scenario.
For the current climate condition, when considering the analysis of the climate associated with the pavements, 3 years in particular were selected from the historical series of precipitations of the Pici pluviometric station (Figure 3). The selection include a year with above average rainfall, a year below average and, finally, a year close to average, these being 1994, 2013 and 2018, respectively.

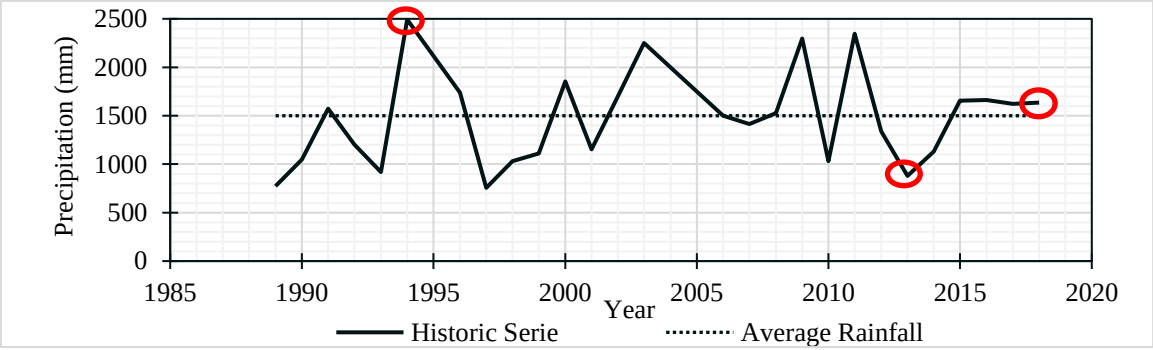

Figure 3. Historical series of rainfall registered by the Pici pluviometric station

2.2. Hydrological Model

The hydrological model was used to characterize the flow and infiltration conditions for the different roadway surfaces. As a hypothesis it was assumed that during the rain event (Figure 4), part of the precipitation (i) became direct runoff (q), and part became infiltration (f), as described by the following equations:

$$q = C.i \quad (2)$$

$$f = (1 - C).i \quad (3)$$

Where: C is the dimensionless runoff coefficient.

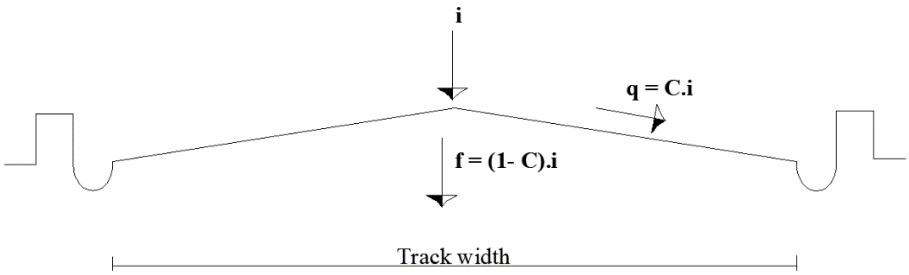

Figure 4. Model of runoff and infiltration of the pavement

For the geometric model of pavement surfaces, a standard 6m road cross section was defined, as indicated in Figure 5. Based on the work of [18], it was adopted a dimensionless runoff coefficient (C) of 0.95 for the part with an asphalt surface course and a coefficient of 0.30 for the part without such surface course, i.e., the roadway shoulder. Four shoulder conditions with different widths or L dimensions were considered (Figure 5): (i) without shoulder (0m); (ii) 0.5m; (iii) 1.0m; and (iv) 1.5m. As for the pavement layers, base and sub-base were 15cm thick each, and three different asphalt surface course thicknesses were considered: ST (surface treatment) with 2cm, AC (asphalt concrete) with either 5cm or 10cm.

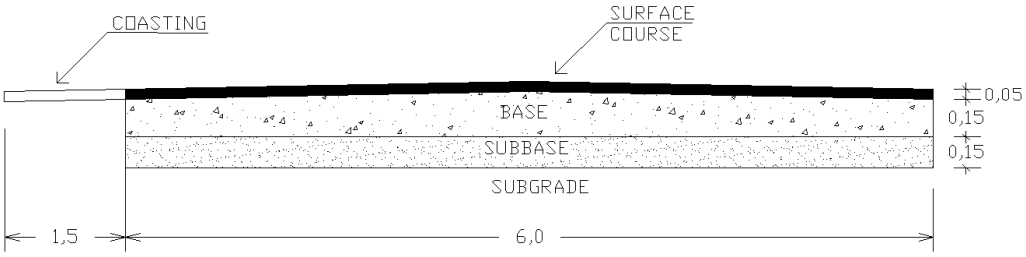

Figure 5. Geometry studied - dimensions in meters

2.3. Flow Model in Unsaturated Porous Media

The climate of the studied region is tropical, ranging from humid to semi-arid. Under such conditions, MRF pavements spend part of their lifespan subjected to an unsaturated condition, with the asphalt surface course also functioning as a waterproofing barrier that makes it difficult for water to infiltrate to the lower layers. This means that the flow modeling must consider the initial unsaturated condition of the pavement layers, given that the fluids present in the voids of the granular structure modify its hydraulic and mechanical properties.

Rocscience's Slide 8.0 program was used for the flow model in transient and unsaturated medium. Subsequently, the finite element method (MEF) was used for modelling, considering input data such as the saturated hydraulic conductivity of the materials (ks), the hydraulic conductivity curve, and the retention curve. For the pavement base, sub-base and subgrade, 3-soil characterizations from [19] were used with data on compaction, CBR (California Support Index), and RM (Resilience Module) tests on MRF soils. Table 1 and Figure 6 show the soil characterization. The subgrade layer was characterized according to AASHTO as an A-2-4 soil, which are boulders or silty or clayey sands, and according to the work of [20] they represent approximately 50% of the MRF soils.

Table 1. Soil characterization

Structure	w_{ot} (%)	$\rho_{smáx}$ (g/cm³)	E	N	LL	LP	AASHTO
Base	6.1	2.273	0.254	0.202	NP	NP	A-1-a
Sub-base	8.6	1.985	0.290	0.225	NP	NP	A-2-4
Subgrade	8.3	1.977	0.280	0.219	NP	NP	A-2-4

Source: Adapted from [17]

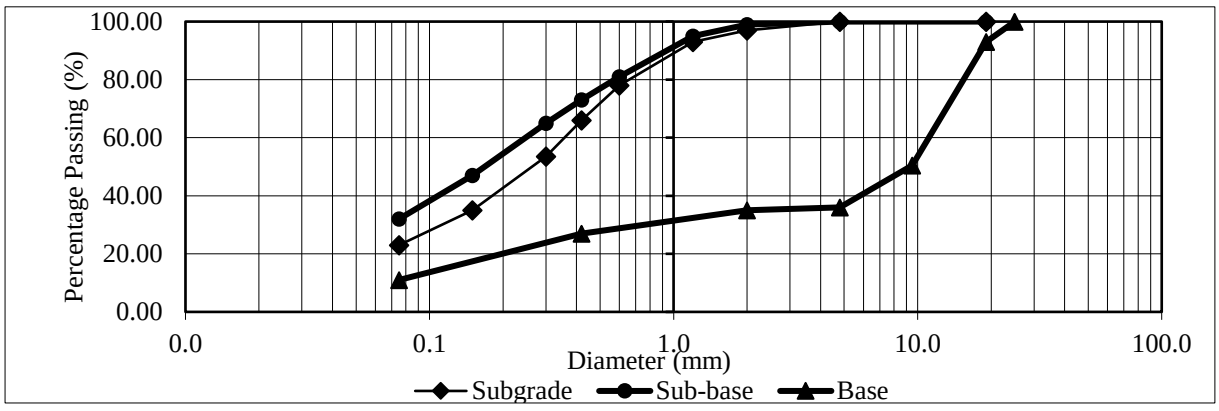

Figure 6. Gradation curves of the pavement soils. Source: Adapted from [19]

As in the work of [17], permeability tests were performed for the base, sub-base and subgrade soils, and the hydraulic conductivity was estimated by Chapuis' empirical equation (2004) for granular materials ([21]):

$$k\ (cm/s) = 2.4622 * \left[D_{ef}^2 \frac{e^3}{(1+e)}\right]^{0,7825} \quad (4)$$

Where: *e* is the void index, and D*ef* is the effective diameter.

For the hydraulic conductivity of the asphalt surface course, two types were investigated: asphalt concrete (AC) and surface treatment by penetration (STP). As mentioned by [22] and [23], STP is one of the most used pavement surfaces in the state of Ceará, covering approximately 63% of its entire paved network.

[24] analyzed the flow conditions in six asphalt mixtures with different air voids (Vv). Among the analyzed mixtures, it was decided to use the AC with 4% air voids. Kozeny – Carman equation (Equation 5) was used to predict ks of the STP, a technique also found in the work of [25], who applied this equation to predict the permeability of different mixtures.

$$ks\ (m/s) = \frac{C.n^3.D_s^2}{(1-n)^2}.\frac{\gamma}{\mu} \quad (5)$$

Where: k_S = permeability coefficient of the saturated medium (m/s); C = form factor equal to 1/180 for spherical particles; D_S = average particle diameter; n = percentage of voids in the air; $\gamma = 9.79 kN/m^3$, unit weight of the fluid (water at 20 ° C); and μ = fluid viscosity, equal to 10^{-3}kg/(m.s) for water.

Based on the above equations, hydraulic conductivities of the different materials that make up the pavement layers were used in the modeling (Table 2).

Table 2. Coefficient of permeability of the pavement materials

Material	Hydraulic Conductivity (m/s)
Asphalt Surface Course - AC	8.82×10^{-7}
Base	1.42×10^{-5}
Sub-base	9.32×10^{-6}
Subgrade	9.53×10^{-6}

To estimate the material retention curves, it was used the methodology by [26], which predicts soil granulometry data. The particle size distribution curve can be divided into n arbitrary fractions, with an average pore diameter and an idealized retention curve for each fraction. This curve is determined by its air intake value and by total and abrupt drainage ([26]; [27]).

From the equations presented and the characterization of the soils by [19], it was possible to estimate the retention curves for the subgrade, subbase and base soils, as shown in Figure 7. The methodology of [26] was applied by [28] to a sandy-silty soil in the city of Fortaleza, presenting forecasts that are quite consistent with the results of the laboratory tests.

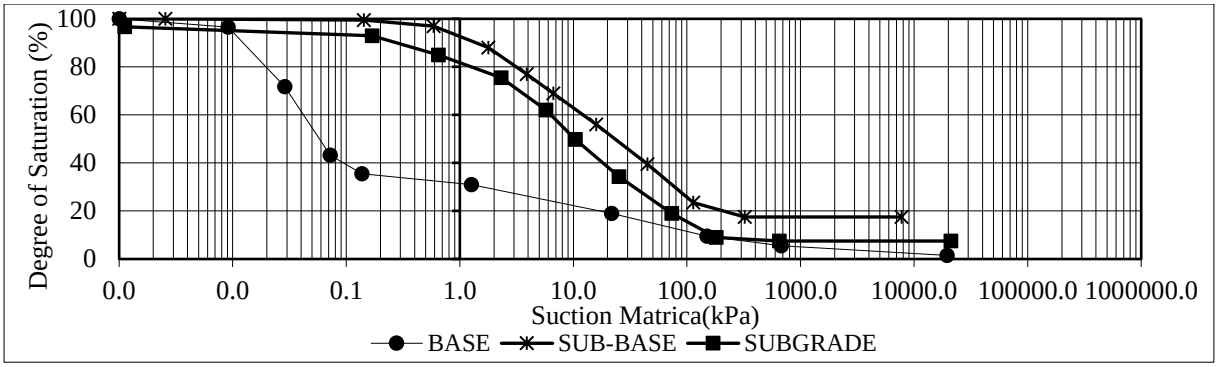

Figure 1. Characteristic Curve

The curves of the hydraulic conductivity function were generated based on the proposal by [29] and [30], which correlates the suction data with volumetric moisture and the hydraulic conductivity function:

$$\theta = \theta_s \left[\frac{ln\left(1+\frac{\psi}{\psi_r}\right)}{ln(1+\frac{1000000}{\psi_r})} \right]^m \left\{ \frac{1}{ln(e+\frac{\psi}{a})^n} \right\} \quad (6)$$

Where: θs is the saturation volumetric moisture; ψ is suction (kPa); ψ_r is the total suction (kPa) that corresponds to residual volumetric moisture (θ_r); a is the coefficient of the soil that relates to the air intake value (kPa); e is the Napierian number; n is the soil parameter that controls the slope of the inflection point of the characteristic curve; and m is the parameter that is related to the residual soil moisture.

Another important aspect of the flow modeling in non-saturated porous medium is the definition of the water level depth. It was used the results of [31], who mapped the wells of the MRF. Groundwater conditions of 3.0m, 3.5m, 4.0m and 4.5m were considered, each representative of the different geological regions of the MRF.

In flow modeling it is necessary to define the initial condition. It was defined that at time t = 0, the pavement soil layers would be under optimal moisture. As it is not possible to define a moisture boundary condition in the software, the volumetric moisture corresponding to the optimal gravimetric moisture (optimum moisture of the compaction test) was calculated.

2.4. Pavement Stiffness Model

For the pavement stiffness model, [32] representative equation of the RM (Equation 4) was adapted to incorporate the variation in moisture of the material. The work of [33] indicates that the use of the exponential function (e^x) for the RM calculation, in a given moisture content, has a good correlation and, therefore, Equation 7 was adapted to Equation 8:

$$RM = k1.\ \sigma_3^{k2}.\ \Delta\sigma^{k3} \quad (7)$$

$$RM = k1.\ \sigma 3^{k2}.\ \Delta\sigma^{k3}.e^{k4.(\Delta w)} \quad (8)$$

Where: k1, k2, k3, k4 are regression coefficients; Δw: moisture variation in relation to the optimum compaction moisture; σ3 is the confining stress; Δσ is the deviation stress. Linear regression was used to obtain k1, k2, k3, k4, and the stresses considered in [19] were used to obtain the RM results according to the equations indicated in Table 3.

Table 3. Equations of RM characteristics for each moisture

Structure	Moisture variation		
	-2%	**0**	**2%**
Subgrade	$188.\theta^{0,738}.\tau_{oct}^{-0,461}$ (R^2 =0,83)	$154.\theta^{0,787}.\tau_{oct}^{-0,518}$ (R^2 =0,82)	$149.\theta^{0,603}.\tau_{oct}^{-0,343}$ (R^2 =0,75)

Subbase	$268.\theta^{0,488}.\tau_{oct}^{-0,542}$ (R^2 =0,75)	$197.\theta^{0,640}.\tau_{oct}^{-0,399}$($R^2$ =0,81)	$143.\theta^{0,682}.\tau_{oct}^{-0,520}$($R^2$ =0,71)
Base	$486.\theta^{0,682}.\tau_{oct}^{-0,316}$ (R^2 =0,79)	$378.\theta^{-0,037}.\tau_{oct}^{-0,028}$($R^2$ =0,60)	$253.\theta^{0,454}.\tau_{oct}^{-0,300}$($R^2$ =0,50)

Adapted from [19]

2.4.1. Residue Analysis

For the stiffness model developed in this work, a residue (error) analysis was performed to analyze the fit of the residues to a probability distribution. This produces a model that allows the prediction of the phenomenon, considering its variability and reliability through the levels and confidence intervals. Residues were calculated using the following expression:

$$d = RM_{test} - RM_{model} \tag{9}$$

Where: d = residue between the measured value and the value calculated by the predictive model; RM_{test} = test value; RM_{model} = value calculated by the model.

For the determination of the confidence interval, it was assumed the calculated residuals followed a Normal Probability Distribution. This hypothesis was confirmed by means of an adherence test in the distribution of model residues. Given the normal conditions of the waste distribution curves, the confidence intervals for the residual means were determined, considering a confidence level of $(1 - \alpha)$, calculated as:

$$d - z_{\alpha/2}.\frac{\sigma}{\sqrt{n}} \leq RM_{test} - RM_{model} \leq d + z_{\alpha/2}.\frac{\sigma}{\sqrt{n}} \tag{10}$$

Where: d = arithmetic mean of the deviations calculated for the model; $z_{\alpha/2}$ = Normal distribution random variable, for which the probability of occurrence of a value $d \leq (1 - \alpha)$; σ = sample standard deviation; n = sample size.

Equation 10 can be simplified as follows:

$$RM_{model} + LL \leq RM_{test} \leq UL + RM_{model} \tag{11}$$

Where: LL= lower limit of the confidence interval; UL = upper limit of the confidence interval.

In this way, it is possible to determine the interval in which the value of the test (RM_{test}) of the resilience module is found, from the value that was calculated (RM_{model}) by the model, which is at a confidence level of $(1 - \alpha)$.

2.5. Performance Analysis

To calculate stresses, deformations, displacements and damage, simulations were performed using CAP3D-D (Computational Analysis of Pavements - 3D, which is an asphalt pavement design program, and the CAP3D program ([34]), which is a structural analysis program based on the MEF. The performance analysis is made using the estimates of the most evident structural distresses in asphalt roadways, i.e., permanent deformation and cracking. In CAP3D-D it is possible to make these estimates for the period of interest (months, years, or pavement service life) using performance prediction equations (% of cracked area and permanent deformation). The equation used in the software is discusses in [4].

For the performance analysis of the investigated pavements, the following parameters were used as input data for CAP3D-D:

- Track start date: Jan/2019;

- Initial traffic (N): 1.0×10^6;

- Speed: 60km/h;

- Traffic growth rate: 2.0% (exponential model);

- Structure composed of 3 layers, in addition to the subgrade, all with Poisson's ratio assumed to be 0.35, and thickness and stiffness as previously presented;

- Temperature: 27°C (estimated from INMET data for the average temperature of the city of Fortaleza). In this research, it was decided to consider the constant average temperature, with the objective of analyzing the influence of precipitation only on the pavement performance;

- Master mix curve data: a = 1.19; b = 3.29; d = 0.9130; g = 0.51; α1= 0.00121; α2 = -0.1780; α3 = 3.0800 (according to [4]);

- Data of the fatigue life curve by diametrical compression (CD): K1 = 3.10-11; K2 = -3.535 (according to [4]);

- TD fatigue life curve data of the mixture with CAP 65/90 and Maximum Nominal Size (TMN) de 19,1mm: α = 3,43; C11 = 0.001530; C12 = 0.528; Δ = -1.211; Y = 3709564; β = -0.08 (according to [4]);

- Wheel radius: 0.108m;

- Load per wheel: -20.5kN.

III. RESULTS

3.1. Climate and Hydrological Model

As previously mentioned, 3 years from the historical precipitation series were selected to build the climate model: 1994 (above average rainfall), 2013 (below average rainfall), and 2018 (average rainfall). For the hydrological model, infiltration estimates were calculated using Equation 3, which considers the daily rainfall for each of the years analyzed, and the surface conditions of the terrain (with and without asphalt surface course). Figure 8 shows the daily infiltration values, calculated for the historical precipitation series for 2018. The infiltrations in the asphalt surface course part are much smaller than those in the areas without surface course, due to the flow coefficient adopted.

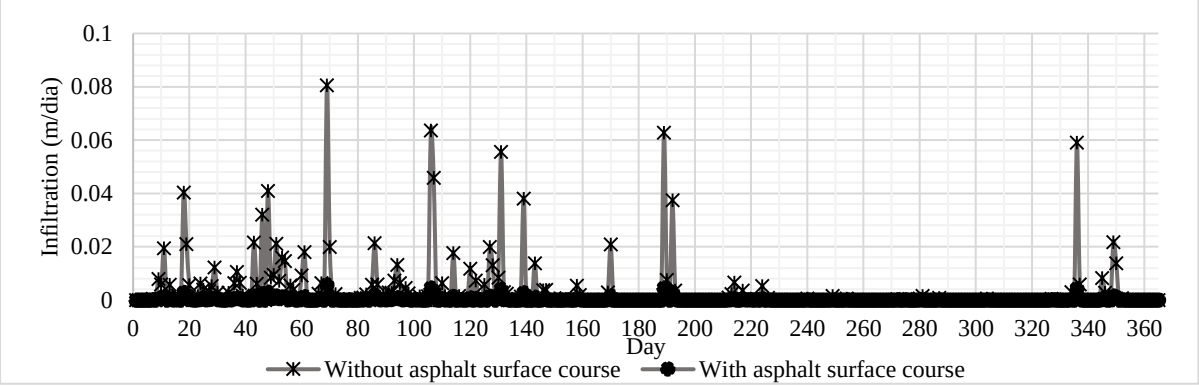

Figure 8. Infiltration for the year with average rainfall: 2018

3.2. Flow Model in Unsaturated Porous Media

Considering the different shoulder conditions (0.0m; 0.5m; 1.0m; 1.5m), the water level depths (3.0m; 3.5m; 4.0m; 4.5m), the varied thicknesses of asphalt surface courses (2.0 cm; 5.0 cm; 10.0 cm), and the 3 rainy periods (above average, below average, close to average), a total of 144 scenarios were modeled. To carry out a comparative analysis of the volumetric moisture variation between the different situations, the following parameters are varied: surface course thickness, variations in water level, and shoulder conditions.

3.2.1. Surface Course Thickness

The modeling results indicate a small distinction between the values for the same water level, precipitations/infiltration, and shoulder conditions given variation in the thickness of the asphalt surface

course. Even in above-average rainfall conditions and for pavements without shoulders (worst scenario), the difference in volumetric moisture for the pavement layers, considering the different thicknesses, is at most 2%. In the following analyzes the results are presented using the 5cm surface course thickness mark, as it represents the intermediate scenario among the 3 investigated.

3.2.2. Water Level Conditions

The modeling of transient flow in unsaturated porous medium indicated that the depth of the water level is an important factor in the analysis. The distance from the pavement layers to the groundwater directly affects soil moisture conditions, as well as variations in the surface climate (rainfall).

Figure 9 shows the variation of the monthly average volumetric moisture in the base layer, for a pavement subjected to above average rainfall conditions (year 1994). It is observed that for the condition without shoulder there is a much greater monthly variability than for the condition with 1.5m shoulder. In the situation without shoulders and for all water levels (WL in the legend) analyzed, during the months of more intense rain (March, April and May), the base layer remains with moisture above the optimum level. In this same period, it is also verified that the layer remains in conditions of saturation equal to 100% given the 3.0m water level condition. This does not occur for pavements with 1.5m of shoulder.

The variability of moisture, even for pavements without shoulders, is small for years with rainfall below the historical average, occurring mainly in the months from February to May. For water levels of 4.0m and 4.5m, the moisture remains below the optimum throughout the year. Pavements with 1.5m shoulders remain with similar monthly average moisture throughout the analyzed period.

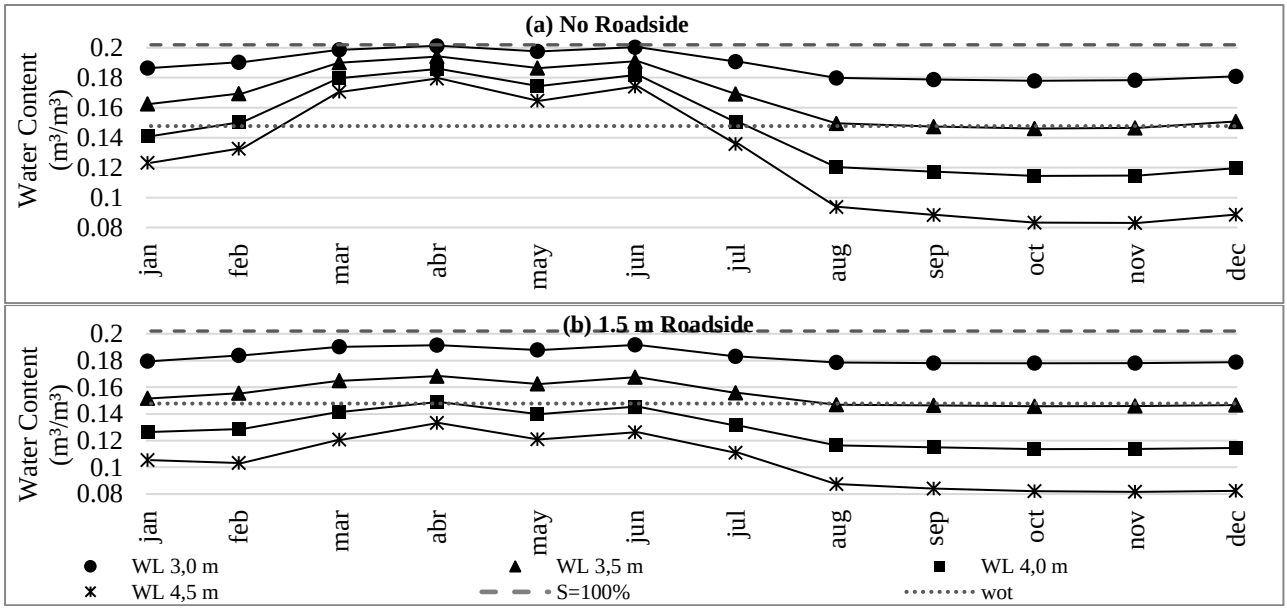

Figure 9. Monthly Average Variation of Volumetric Moisture of the Base Layer: Above Average Precipitation (1994); 5cm coating; (a) No Roadside, (b) 1.5 m Roadside

3.2.3. Roadside Conditions

As expected, the model indicated that the shoulders reduce the moisture variation in the pavement for all scenarios, primarily, for years with above average rainfall. Comparing the observed maximum monthly moisture with the optimum moisture (Figure 10a) showed that, during the years with above-average rainfall, the 1.5m shoulder reduces the moisture variation by another 15%. For years with below-average rainfall, this reduction is approximately 10%.

Making the same comparative analysis for regions with water level at 4.0m depth (Figure 10b), pavements with 1.5m shoulder present a 25% reduction in maximum moisture compared to road structures without any shoulder, for years of high rainfall. For years with below-average rainfall, this reduction reaches 15%.

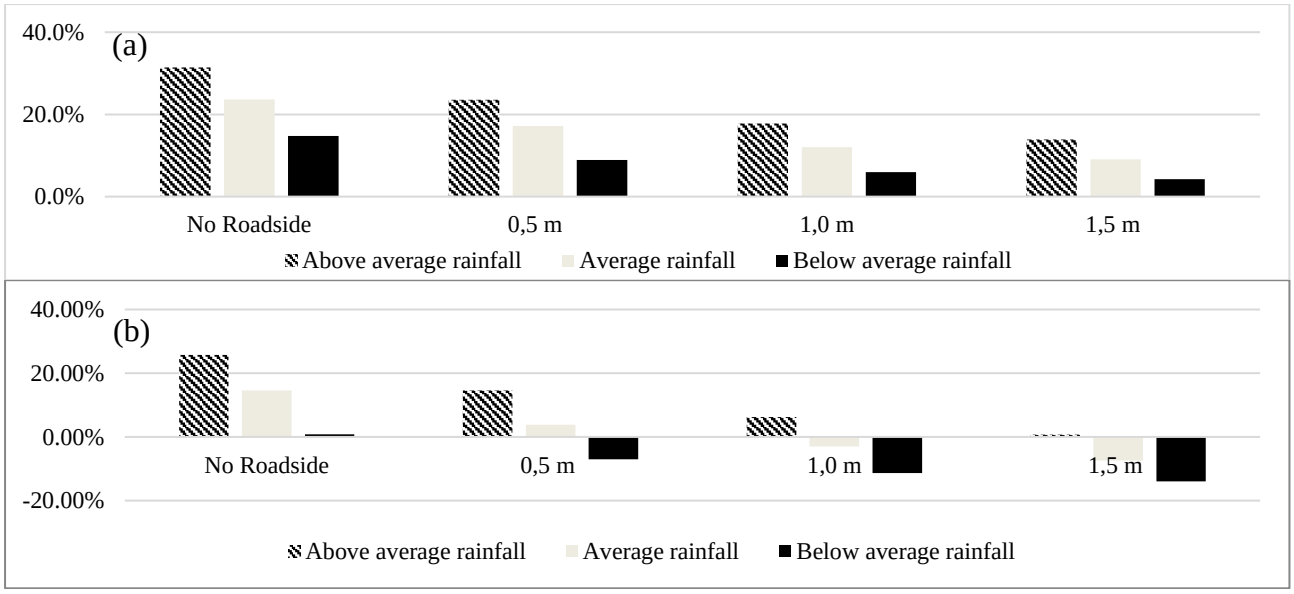

Figure 10. Percentage variation of the Maximum Moisture in relation to the Optimal Moisture: 5cm coating; Water level 3.5m (a) Water level 4.0m (b)

3.3. Pavements Stiffness Model

Equation 8 and the results from [19] were used for the stiffness model, which shows the rigidity of the pavement. The k1, k2, k3 e k4 coefficients were obtained by linear regression.

Table 4. Regression coefficients for calculating RM

Layer	k1	k2	k3	k4
Base	741	0.282	-0.118	-0.116
Subbase	474	0.366	-0.359	-0.328
Subgrade	627	0.510	-0.237	-0.101

The correlations for the RM calculated from Equation 5 and the equations by [19] are satisfactory, with determination coefficient (R^2) values for subgrade, subbase and base soils being, respectively, 0.93, 0.87 and 0.77.

Based on the analysis of the residues, it was possible to determine the expressions of the confidence interval for the resilience module test (RM_{test}), as a function of the modeled value (RM_{model}), considering a 95% confidence level for subgrade soils, subbase and base, respectively (values in MPa):

$$RM_{model} - 13.54 \leq RM_{test} \leq 13.55 + RM_{model} \quad (12)$$

$$RM_{model} - 51.12 \leq RM_{test} \leq 67.01 + RM_{model} \quad (12)$$

$$RM_{model} - 34.94 \leq RM_{test} \leq 36.57 + RM_{model} \quad (14)$$

For the RM variations presented below the following were considered: Equation 8, coefficients indicated in Table 4, confining stress of 0.1034MPa, and deviation stress of 0.1861MPa (for comparative purposes only).

Figure 11 shows the variability of RM for the base layer of a pavement without shoulders in a year with above average rainfall. It appears that for water level at 3.0m depth, RM remains with values below the RMoptimum (resilience module for optimal moisture) during the entire period. Even in months of intense rain (January to June), RM values remain between 360 to 390MPa, reaching maximum average of 405MPa in the dry period. Water level conditions at 3.5m show RM variation of more than 100MPa between the rainy period (first half of the year) and the dry period (second half of the year). For

groundwater levels of 4.0 and 4.5m, the second half of the year shows gains in material stiffness, between 6% to 38% in relation to the optimum moisture (water level = 4.5m).

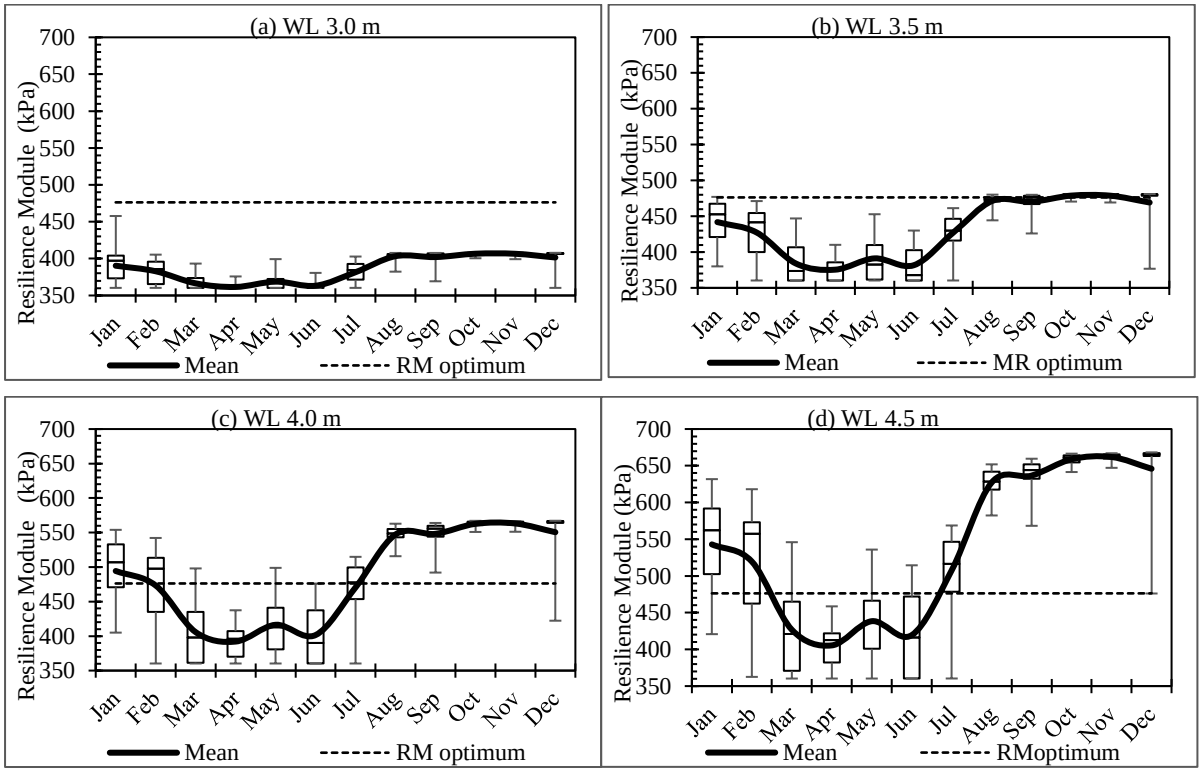

Figure 11. Monthly Variability of the RM of the Base Layer: Above Average Precipitations (1994); 5cm surface course; No Roadside; (a) WL 3.0m, (b) WL 3.5m, (c) WL 4.0m, (d) WL 4.5m

For years with below average rainfall, the results indicate that the RM variability for groundwater at 3.0m depth is even lower than in the previous condition, remaining between 380 to 400MPa in the first semester, reaching maximum values of 405MPa during the dry period. For water level at 3.5m, the RM variation between dry and rainy periods is reduced to 50MPa. Under 4.0m and 4.5m water level conditions, even without shoulders, for dry years, the average monthly RM remains above the optimum throughout the year. However, some events of intense rain, can reduce the daily RM values up to 22% in relation to the MRoptimum.

Analyzing the water level condition at 4.5m, according Figure 12, even in years with intense rain, the 1.5m shoulder ensures that the average monthly RM remains above the optimum. Furthermore, even on days with intense rain, the minimum values observed are within the confidence interval of RMoptimum. Comparing the condition without shoulders, in the periods of greatest precipitation (March, April, May and June), the material's stiffness is reduced to values lower than the optimum condition.

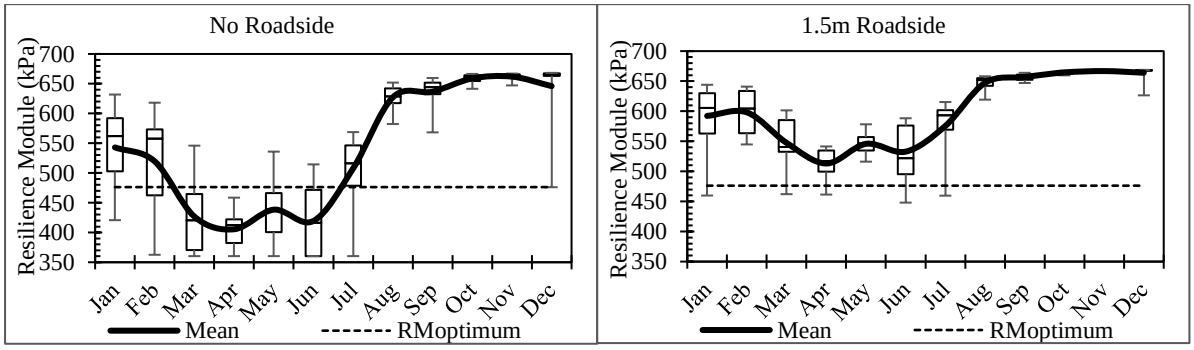

Figure 12. Monthly Variability of the RM of the Base Layer: Above Average Precipitations (1994); 5cm coating; Water level 4.5m; (A) No Roadside, (b) 1.5m Roadside

3.4. Performance Analysis

For the performance analysis, 6 scenarios were selected. CAP3D-D still does not have an implemented routine that considers conditions of RM variability. Therefore, part of the analysis has to be done in a non-automated way, which generates a high computational time (60 times greater when compared to modeling without considering the RM variability, in a computer with a simple processor). The scenarios are shown in Table 5. The surface course thickness (5cm) and the water level (3.5m) were fixed. For damage estimates, cracked area and permanent deformation, the conditions of the shoulder were varied (without and with 1.5m shoulder) and rainfall (below average, average, and above average).

Table 5 - Modeled Scenario

Roadside	Precipitation		
	Below Average	Average	Above average
0.0 m	Scenario 1	Scenario 2	Scenario 3
1.5 m	Scenario 4	Scenario 5	Scenario 6

The percentage estimates of cracked area for the 6 scenarios are presented in Figure 13. As expected, the worst is scenario 3 (above average rainfall, without shoulder), with higher damage and cracked area values. The best scenario, with results close to the optimal moisture condition, is scenario 4 (below average rainfall, with shoulders).

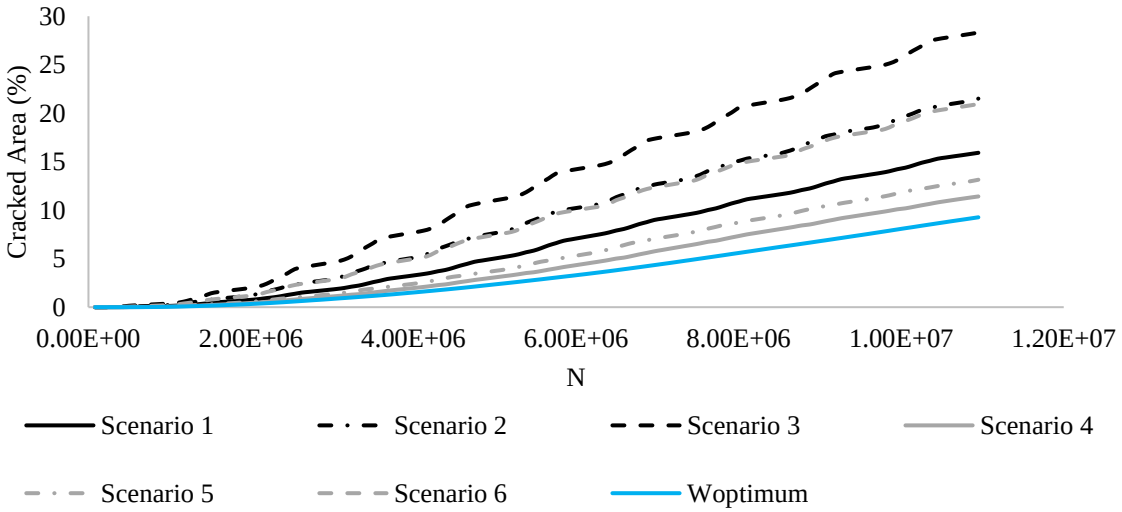

Figure 2. Percentage of Cracked Area

In order to identify the change in the service life of structures analyzed in the aforementioned scenarios, it was identified the period (years) needed for 10% of the cracked area to be reached. These results are shown in Figure 14. Comparing the above-average precipitation years (Scenario 3 and Scenario 6) one can observe that the shoulder increases the period to reach 10% of cracked area in up to 1.3 years. Considering the years with average rainfall (Scenario 2 and Scenario 5), this increase is 2.8 years. For the drier years (Scenario 1 and Scenario 4), the increase is 2.3 years.

Comparing the scenarios of the integrated model with the condition of the constant RM (determined in the condition of optimum moisture), the graph shows that the percentage reduction of time to reach 10% of cracked area for pavements with shoulders varies from 31% to 56%. This reduction for conditions with 1.5m of shoulder ranges from 8.3% to 42.5%. It is observed in all scenarios, a reduction in service life that ranges from 1 to 5.6 years when compared to the mechanistic-empirical design with RMoptimum.

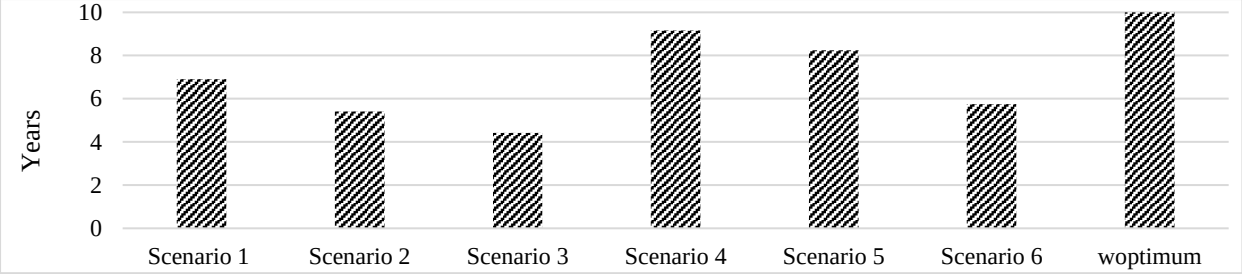

Figure 14 - Period to reach 10% of Cracked Area

3.5. Climate Change Scenarios

For climate change scenarios, Figure 15 shows the frequency distributions of rainfall for the RCPs (Representative Concentration Pathways) 8.5 and 4.5 projections. The RCP 8.5 scenario is the most conservative and pessimistic, however, according to [35], it is the one most likely to happen. In this scenario, a higher frequency of years with rainfall below the historical average is observed for all models analyzed. Models BCC-CSM1 (RCP 8.5), CanESM2 (RCP 8.5) and CESM1-CAM5 (RCP 8.5) also point to a reduction in minimum rainfall.

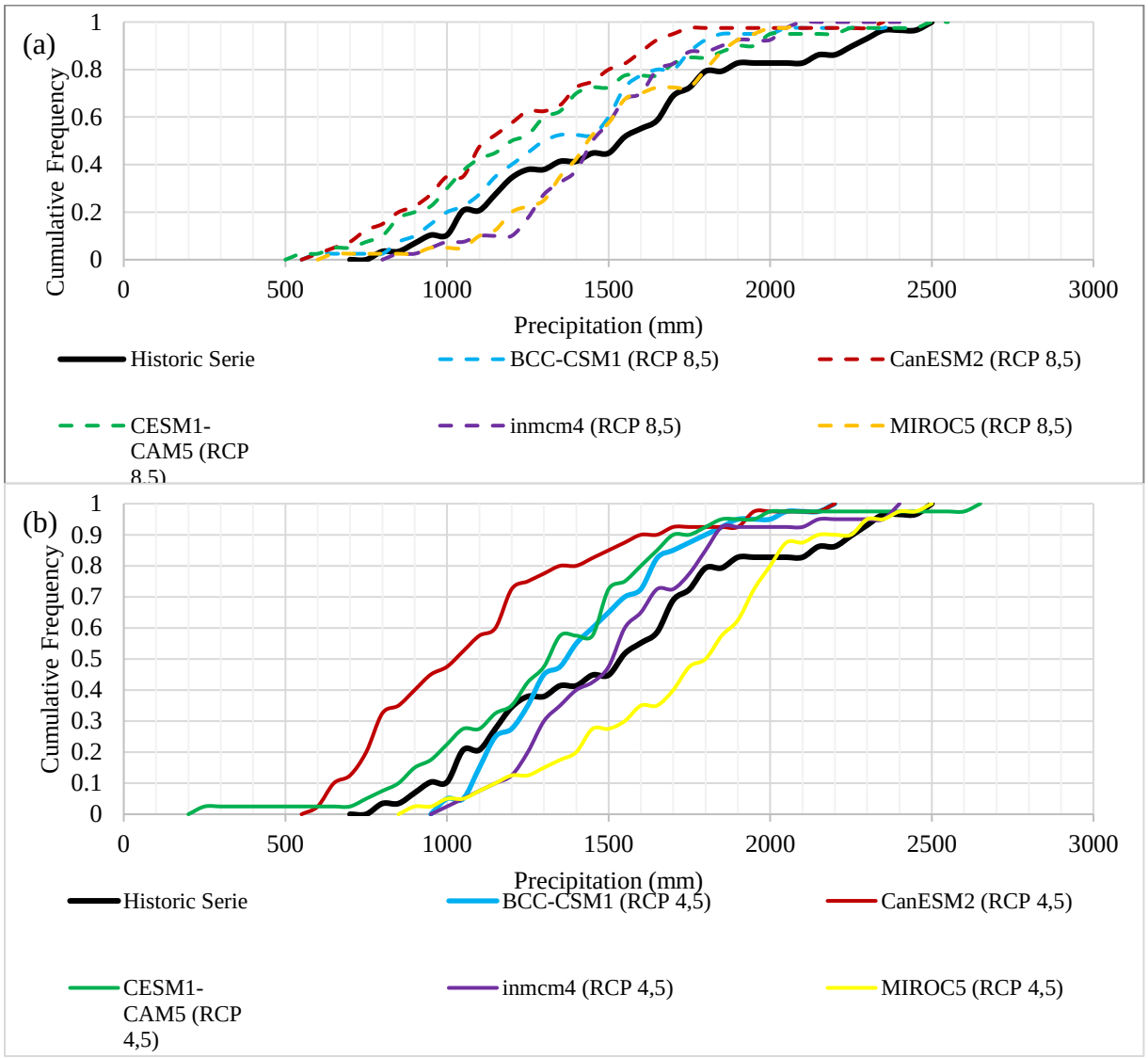

Figure 15. Accumulated frequency of rainfall for 21st century climate change scenarios (2031-2070) - RCP 8.5 (a); RCP 4.5 (b)

The RCP 4.5 scenario is associated with a low greenhouse gas emission rate (compared to RCP 8.5) and assumes that there will be a regular number of political and environmental measures applied by countries ([35]). Most models, for this scenario, indicate that for the MRF there should also be a higher frequency of years with rainfall below the historical average. The MIROC5 model (RCP 4.5) projects a higher frequency of rainfall above the historical average.

Figure 16 shows the distribution of rainfall in the historical series and climate change models for the 21st century (2031 to 2070). To compare and analyze the results, the minimum, average and maximum precipitation anomalies were calculated according to Equation 1 (Table 6).

The anomalies of minimum precipitation for the projections of the scenarios RCP 8.5 and RCP 4.5 are divergent. For RCP 8.5, the minimum precipitation anomalies range from -23% to 9%. However, 4 of the 5 models indicate negative anomalies. As for RCP 4.5, the variability of anomalies is much greater, from -73% to 29%, presenting 3 models with positive anomalies.

For average rainfall anomalies, all RCP 8.5 projections show negative values (-2% to 22%). In the RCP 4.5 scenarios, these anomalies for Model inmcm4 indicate that there will be no change, while Models BCC-CSM1, CanESM2, CESM1-CAM5 present negative anomalies and Model MIROC5 is the only one that indicates positive anomaly values.

In the period from 2031 to 2070, the projections of the maximum precipitation scenarios RCP 4.5 and RCP 8.5 are similar. The models indicate anomaly values between -17% and 5%.

Table 6. Maximum, Average and Minimum Precipitation Anomalies for 21st Century Climate Change Scenarios (2031-2070)

	BCC-CSM1		**CanESM2**		**CESM1-CAM5**		**inmcm4**		**MIROC5**	
	RCP 8.5	**RCP 4.5**	**RCP 8.5**	**RCP 4.5**	**RCP 8.5**	**RCP 4.5**	**RCP 8.5**	**RCP 4.5**	**RCP 8.5**	**RCP 4.5**
Minimum	**-21%**	**27%**	**-23%**	**-23%**	**-28%**	**-73%**	**9%**	**29%**	**-15%**	**19%**
Average	**-11%**	**-8%**	**-22%**	**-29%**	**-16%**	**-14%**	**-2%**	**0%**	**-3%**	**13%**
Maximum	**-5%**	**-14%**	**-6%**	**-14%**	**4%**	**5%**	**-2%**	**-5%**	**-17%**	**-1%**

In general, most climatic scenarios indicate that for the 21st century, the pavements will be subjected to a higher frequency of years with below average rainfall, indicating a more frequent occurrences of infiltration scenarios. Maximum precipitations can reach reductions of up to -17% and a maximum increase of 5%. However, most models indicate that these should occur less frequently. Thus, the performance analysis of scenarios 3 and 6 are less likely to happen.

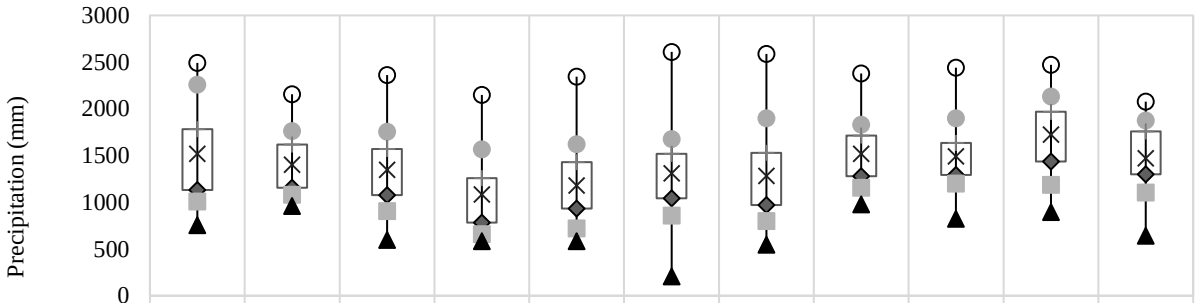

	Série Histórica	BCC-CSM1 (RCP 4,5)	BCC-CSM1 (RCP 8,5)	CanESM2 (RCP 4,5)	CanESM2 (RCP 8,5)	CESM1-CAM5 (RCP 4,5)	CESM1-CAM5 (RCP 8,5)	inmcm4 (RCP 4,5)	inmcm4 (RCP 8,5)	MIROC5 (RCP 4,5)	MIROC5 (RCP 8,5)
◆1° Quartile	1131.50	1155.78	1076.29	783.34	934.94	1042.32	970.45	1280.93	1291.63	1437.44	1301.10
■10° Percentile	1008.62	1079.72	906.41	658.34	721.41	857.53	801.20	1157.54	1199.67	1185.91	1104.56
▲Minimum	756.10	959.89	599.28	582.40	585.75	206.72	546.44	976.29	824.74	896.85	643.76
×Average	1520.48	1403.79	1347.10	1083.03	1181.64	1310.23	1282.41	1517.55	1490.24	1724.65	1469.74
○Maximum	2492.60	2155.37	2362.96	2151.01	2344.05	2610.01	2587.60	2380.09	2438.88	2472.03	2078.14
●90° Percentile	2258.26	1763.09	1756.28	1565.98	1622.10	1676.43	1899.80	1829.63	1899.86	2133.16	1875.46
+3° Quartile	1783.40	1618.44	1570.95	1258.28	1428.44	1519.97	1529.09	1712.68	1637.02	1969.54	1757.39

Figure 16. Boxplot graph: historical series and 21st century climate change scenarios (2031-2070)

IV. CONCLUSIONS

This work presented a methodology that allows integrated management of civil infrastructure. The research showed that it is possible to produce a structure linking climate, hydrology and pavement subsystems, allowing for a joint analysis of the results through models and integration known variables that can be used by technicians and academics.

Considering the scenarios studied for the integrated model, the roadway performance analysis for the MRF showed that the presence of pavement shoulder (1.5m) increases the 10% of cracked area to an upward limit of 2.8 years, when compared to a condition without shoulder. It is possible to verify, in all scenarios, that the presence of the shoulder increases the performance and, consequently, the pavement service life. In addition, shoulders also increase road safety, reducing traffic accidents. In all scenarios of the integrated model, a reduction in service life was observed, ranging from 1 to 5.6 years when compared to the mechanistic-empirical design using MRoptimum. Without the integrated methodology, the project is under designed.

Years with above average rainfall reduce pavement life from 42.5% to 55.8%. For years of average precipitation, the decrease varies from 17.5% to 45.8%, and for years below the average it is from 8.3% to 30.8%. Climate change models generally indicate that for the 21st century (2031-2070), MRF pavements will be subjected to a higher frequency of years with below average rainfall. However, most models indicate that these should occur less frequently.

The results for water level of 4.5m and pavement with shoulders suggest that even in years of high rainfall, the moisture in the pavement layers remains below the optimum throughout the year. This study also shows that pavements, mainly those of low cost in the region, with groundwater below 4.5m, can incorporate gains in stiffness in the granular layers for moistures below optimum levels.

Based on the results, it is possible to verify that the integrated methodology provides gains in comparison to the traditional methodologies of pavement design and management. As advantages of the proposed methodology one can mention that (i) it allows an overview of the subsystems as a whole, enabling the characterization of the environment closer to the real condition; (ii) it enables the identification of pavements that will be subjected to moisture variations above or below the optimum; and (iii) it makes it possible to predict scenarios of climate change and to assist in the decision-making of projects for the 21st century (2031-2070).

REFERENCES

[1]. Steffen, W.; Grinevald, J.; Crutzen, P.; McNeill, J. (2011) The Anthropocene: conceptual and historical perspectives. Philosophical Transactions of The Royal Society, p. 842-867. DOI: https://doi.org/10.1098/rsta.2010.0327

[2]. Hamilton, C.; Bonneuil, C.; Gemenne, F. (2015) The Anthropocene and the Global Environmental Crisis. London/New York: Routledge. ISBN 9781138821248

[3]. Meybeck, M. (2003) Global analysis of river systems: from earth system controls to Anthropocene controls. Philosophical Transactions of the Royal Academy B, p. 1935-1955. DOI: 10.1098/rstb.2003.1379

[4]. Santiago, L. S.; Silva, S. A. T.; Soares, J. B. (2018) Determinação do dano em pavimentos asfálticos por meio da combinação do modelo S-VECD com análises elásticas. Revista Transportes (Rio de Janeiro), v. 26, p. 31-43. DOI: https://doi.org/10.14295/transportes.v26i2.1446

[5]. Motta, L. M. G.; Leite, L. F. M.; Franco, F. A. C. P.; Silva, C. F. S. C.; Medina, J. (2018) Execução de estudos e pesquisa para elaboração de método mecanístico - empírico de dimensionamento de pavimentos asfálticos. Convênio UFRJ/DNIT.

[6]. Mallick, R. B.; Radzicki, M. J.; Daniel, J. S.; Jacobs, J. M. (2014) Use of System Dynamics to Understand Long-Term Impact of Climate Change on Pavement Performance and Maintenance Cost. Transportation Research Record: Journal of the Transportation Research Board, 2455(1). DOI: https://doi.org/10.3141/2455-01

[7]. Underwood, B. S.; Guido, Z.; Gudipudi, P.; Feinberg, Y. (2017) Increased costs to US pavement infrastructure from future temperature rise. Nature Climate Change, [s.l.], v. 7, n. 10, p.704-707. DOI: https://doi.org/10.1038/nclimate3390

[8]. Underwood, B. S. (2019) A method to select general circulation models for pavement performance evaluation. International Journal of Pavement Engineering, [s.l.], p. 1-13. DOI: https://doi.org/10.1080/10298436.2019.1580365

[9]. Kim, Y.; Eisenberg, D. A.; Bondank, E. N.; Chester, M. V.; Mascaro, G.; Underwood, B. (2017) Fail-safe and safe-to-fail adaptation: decision-making for urban flooding under climate change: decision-making for urban flooding under climate change. Climatic Change, [s.l.], v. 145, n. 3-4, p. 397-412. DOI: https://doi.org/10.1007/s10584-017-2090-1

[10]. Sabóia, M. A. M.; Souza Filho, F. A.; Araújo Júnior, L. M.; Silveira, C. da S. Climate changes impact estimation on urban drainage system located in low latitudes districts: a study case in Fortaleza-CE. RBRH, vol. 22(0), 2017. DOI: https://doi.org/10.1590/2318-0331.011716074

[11]. Gudipudi, P. P.; Underwood, B. S.; Zalghout, A. (2017) Impact of climate change on pavement structural performance in the United States. Transportation Research Part D: Transport and Environment, [s.l.], v. 57, p. 172-184. DOI: https://doi.org/10.1016/j.trd.2017.09.022

[12]. Markolf, S. A.; Hoehne, C.; Fraser, A.; Chester, M. V.; Underwood, B. S. (2019) Transportation resilience to climate change and extreme weather events – Beyond risk and robustness. Transport Policy, [s.l.], v. 74, p.174-186. DOI: https://doi.org/10.1016/j.tranpol.2018.11.003

[13]. Stoner, A. M. K.; Daniel, J. S.; Jacobs, J.M; Hayhoe, K.; Scott-Fleming, I. (2019) Quantifying the Impact of Climate Change on Flexible Pavement Performance and Lifetime in the United States. Transportation Research Record: Journal of the Transportation Research Board, v. 2673, n. 1, p.110-122. DOI: https://doi.org/10.1177/0361198118821877

[14]. Silveira, C. S.; Souza Filho, F. A.; Costa, A. C.; Cabral, S. L. (2013) Avaliação de desempenho dos modelos do CMIP5 quanto à representação dos padrões de variação da precipitação no século XX sobre a região Nordeste do Brasil, Amazônia e Bacia do Prata e análise das projeções para o cenário RCP8.5. RBMET – Revista Brasileira de Meteorologia, Vol. 28, n. 3, pp. 317-330. DOI: https://doi.org/10.1590/S0102-77862013000300008

[15]. Silveira, C. S.; Souza Filho, F. A.; Martins, E. S. P. R.; Oliveira, J. L.; Costa, A. C.; Nobrega, M. T.; Souza, S. A.; Silva, R. F. V. (2016) Mudanças climáticas na bacia do rio São Francisco: Uma análise para precipitação e temperatura. RBRH – Revista Brasileira de Recursos Hídricos, Vol. 21, n.2, pp. 416-428. DOI: https://doi.org/10.21168/rbrh.v21n2.p416-428

[16]. Fernandes, W. S. (2012) Avaliação do Impacto das Mudanças Climáticas na Oferta Hídrica da Bacia Hidrográfica do Reservatório Orós Usando os Modelos de Mudanças Climáticas do IPCC-Ar4, Levando em Consideração as Diversas Incertezas Associadas. Tese (Doutorado) - Universidade Federal do Ceará. Fortaleza. <https://repositorio.ufc.br/handle/riufc/3962> (acesso em 02/03/2023)

[17]. Silveira, C. S. et al. (2015) Análise das Projeções de Vazões nas Bacias do Setor Hidroelétrico Brasileiro Usando Fados do IPCC-AR5 para o Século XXI. In: SOUZA FILHO, F. A.; SILVEIRA, C. S. Uso da Informação Climática em Múltiplas Escalas Temporais para o Planejamento do Setor Hidroelétrico Brasileiro. 1. ed. Fortaleza: Expressão Gráfica e Editora, p. 137-159. ISBN 978-85-420-0763-3.

[18]. Porto, R. L. Escoamento Superficial Direto. In: Tucci, C. E. M.; Porto, R. la L.; Barros, M. T. Drenagem Urbana. Porto Alegre: ABRH/Editora da Universidade/UFRGS, 1995.

[19]. Bastos, J. B. S. (2013) Influência da variação da umidade no comportamento de pavimentos da região metropolitana de Fortaleza. Dissertação (Mestrado em Engenharia de Transportes) - Universidade Federal do Ceará. Fortaleza. Disponível em: < https://repositorio.ufc.br/handle/riufc/5627> (acesso em 02/03/2023)

[20]. Ribeiro, A. J. A. (2013) Um Método Para Localização e Estimação das Características Geotécnicas dos Solos da Região Metropolitana de Fortaleza-CE para Fins de Pavimentação. Dissertação (Mestrado) - Universidade Federal do Ceará. Fortaleza. < https://repositorio.ufc.br/handle/riufc/5461> (acesso em 02/03/2023)

[21]. Chapuis, R. P. Predicting the saturated hydraulic conductivity of sand and gravel using effective diameter and void ratio. Canadian Geotechnical Journal, [s.l.], v. 41, n. 5, p.787-795, 2004. Canadian Science Publishing. http://dx.doi.org/10.1139/t04-022.

[22]. Vasconcelos, M. A. G. (2013) Estudo Sobre o Emprego do Cape Seal em Revestimentos Rodoviários do Estado do Ceará. 227 f. Dissertação (Mestrado) - Universidade Federal do Ceará. Fortaleza. < https://repositorio.ufc.br/handle/riufc/7989> (acesso em 02/03/2023)

[23]. Silva, R. C. (2018). Avaliação da Dosagem dos Tratamentos Superficiais por Penetração de Rodovias Baseada na Exsudação e na Perda de Agregados. Dissertação (Mestrado) - Universidade Federal do Ceará. Fortaleza. < https://repositorio.ufc.br/handle/riufc/31541> (acesso em 02/03/2023).

[24]. Ferreira, W. L. G.; Branco, V. T. F. C.; Silva Filho, F. C. (2014) Simulação Numérica do Fluxo D'água em Pavimentos Flexíveis Compostos por Diferentes Misturas Asfálticas. In: ANPET – XXVIII CONGRESSO DE PESQUISA E ENSINO EM TRANSPORTES, Curitiba.

[25]. Masad, E.; Al-Omari, A.; Lytton, R. (2006) Simple Method for Predicting Laboratory and Field Permeability of Hot-Mix Asphalt. Transportation Research Record: Journal of the Transportation Research Board, v. 1970, p.55-63. DOI: https://doi.org/10.1177/0361198106197000010

[26]. Arya, L. M. and Paris, J. F. (1981) A physicoempirical model to predict the soil moisture characteristic from particle-size distribution and bulk density data. Soil Science Soc. Am. J., v. 45, p. 1023-1030, 1981. https://doi.org/10.2136/sssaj1981.03615995004500060004x

[27]. Gitirana Jr., G. F. N.; Camapum de Carvalho, J.; Cordao Neto, M. P. Previsão de curvas características de um perfil de solo colapsível de Brasília utilizando curvas granulométricas. In: XIII Congresso Brasileiro de Mecânica do Solos e Engenharia Geotécnica, Anais, Curitiba, v. I, 6 p, 2005.

[28]. Almeida, M. M. R. (2018) Avaliação de Métodos de Estimativa da Capacidade de Carga de Fundações Diretas em Solos Não Saturados. Dissertação (Mestrado) - Universidade Federal do Ceará. Fortaleza. Disponível em: <https://repositorio.ufc.br/handle/riufc/29818?locale=en> (acesso em 02/03/2023)

[29]. Fredlund, D. G.; Xing, A. (1994) Equations for the Soil-Water Characteristic Curve. Canadian Geotechnical Journal, p. 521-532, 1994. DOI: https://doi.org/10.1139/t94-061

[30]. Fredlund, D. G.; Xing, A.; Huang, S. (1994) Predicting the permeability function for unsaturated soils using the soil–water characteristic curve. Canadian Geotechnical Journal, 31(4), p. 533–546. DOI: https://doi.org/10.1139/t94-062

[31]. Cavalcante, I. N. (1998) Fundamentos Hidrogeológicos para a Gestão Integrada de Recursos Hídricos na Região Metropolitana de Fortaleza Estado do Ceará. Tese (Doutorado) - Universidade de São Paulo, São Paulo. < https://teses.usp.br/teses/disponiveis/44/44133/tde-12112015-140423/pt-br.php> (acesso em 02/03/2023)

[32]. Pezo, R. F. A General Method of Reporting Resilient Modulus Tests of Soils: A Pavement Engineer's Point of View. Presented at the 72nd Annual Meeting of the Transportation Research Board, Washington, D.C., 1993.

[33]. Takeda, M. C. A influência da variação da umidade pós-compactação no comportamento mecânico de solos de rodovias do interior paulista. (2006) Tese (Doutorado) - Escola de Engenharia de São Carlos, Universidade de São Paulo. São Carlos. < https://www.teses.usp.br/teses/disponiveis/18/18143/tde-25112006-225630/pt-br.php> (acesso em 02/03/2023)

[34]. Holanda, A. S.; E. Parente Jr.; T. D. P. Araújo; Melo, L. T. B.; F. Evangelista Jr, F..; Soares, J.B.(2006) Finite Element Modeling of Flexible Pavements. In: Anais XXVII Iberian Latin-American Congress on Computational Methods in Engineering (CILAMCE). Belém, Pará.

[35]. VUUREN, D. P.; EDMONDS, J.; KAINUMA, M.; RIAHI, K.; THOMSON, A.; HIBBARD, K.; ROSE, S. K. The representative concentration pathways: an overview. Climatic Change, v. 109, n. 1-2, p. 5–31, 2011.

AUTHORS

Carla Beatriz Costa de Araújo - Graduated in Civil Engineering from the Federal University of Ceará (2013) - Magna Cum Laude. Master's Degree in Civil Engineering - Concentration Area: Geotechnics from the Federal University of Ceará (2015). PhD in Civil Engineering at the Federal University of Ceará (2019). She worked at Arcadis Logos S/A as a civil engineer and coordinator of the management team of DRENURB (Municipal Urban Drainage Program of Fortaleza). She is currently a professor at the same university working in the area of geotechnics in the Department of Geology.

Francisco de Assis de Souza Filho - Graduated in Civil Engineering from the Federal University of Ceará (1990), master's degree in Hydraulic and Sanitation Engineering from the School of Engineering of São Carlos, University of São Paulo (1995) and PhD in Civil Engineering from the Polytechnic School of the University of São Paulo (2006) . He is currently a professor at the Department of Hydraulic and Environmental Engineering at the Federal University of Ceará (2008-current). He coordinates the Research Group "Climate Risk Management for Water Sustainability" at UFC. He is Research Associate at the Columbia Water Center at Columbia University in New York (2006-current). He serves as an editor and reviewer for several national and international journals.

Jorge Barbosa Soares - Civil Engineer by UFC (1991). MSc. (1994) and Ph.D. (1997) in Civil Engineering from Texas A&M University. He is a Full Professor at UFC, Director of Innovation at FUNCAP since 2015, and on the Advisory Committee of CNPq (CA-EC) since 2018, he has been Coordinator of Graduate Studies and Head of the Department of Transport Engineering, and Director of Research at UFC Technology Center. He coordinates the Laboratory of Mechanics of Pavements and the National Institute of Science and Technology in Characterization of Materials for Infrastructure (INCT-Infra) of CNPq. He is Director of Research and Innovation at the UFC's Artificial Intelligence Reference Center (CRIA).

Samuel de Almeida Torquato e Silva - PhD in Geotechnics from the University of Brasília, Master in Transport Engineering PETRAN/UFC (2017), Civil Engineer graduated from the Federal University of Ceará (2014). He has research experience in computational mechanics focused on Transport Infrastructure. He has worked as a researcher for Petrobras' Asphalt Thematic Network, for Infralab (UnB) and for road management consulting companies and the development of infrastructure projects.